1984

Sondrestrom Overview

Vincent B. Wickwar
Utah State University

J D. Kelly

O de la Beaujardiere

C A. Leger

F Steenstrup

C H. Dawson

Recommended Citation
Wickwar, V. B., J. D. Kelly, O. de la Beaujardière, C. A. Leger, F. Steenstrup, and C. H. Dawson (1984), Sondrestrom overview, Geophys. Res. Lett., 11(9), 883–886, doi:10.1029/GL011i009p00883.

GEOPHYSICAL RESEARCH LETTERS, VOL. 1, NO. 9, PAGES 883-886, SEPTEMBER 1984

SONDRESTROM OVERVIEW

V. B. Wickwar, J. D. Kelly, O. de la Beaujardière, C. A. Leger, F. Steenstrup, and C. H. Dawson,

Radio Physics Laboratory, SRI International

Abstract. This overview of the Sondrestrom radar provides background material to help understand the early scientific results discussed in the following series of papers. It describes the geophysical region probed by the radar, the data acquisition procedure, and the extensive set of physical parameters derived.

Introduction

Located in Sondre Stromfjord, Greenland (66.987 N, 50.949 W), the incoherent-scatter radar (formerly the Chatanika radar) is the very high-latitude anchor (74° invariant) of a meridional chain of four radars stretching a quarter of the way around the earth to the magnetic equator. It can now probe the region below the magnetospheric cusp near noon, the polar cap near midnight, and the poleward portion of the auroral oval in between. It is, therefore, in a prime location to study a wide variety of interactions among the magnetosphere, ionosphere and neutral atmosphere, and the effects of the solar wind and interplantary magnetic field on these interactions. Considerable opportunities also exist for correlative and complementary observations with, among others, the collocated optical facility operated by the University of Michigan and the network of magnetometers operated by the Danish Meteorological Institute.

Geophysical Context of the Observations

To plan experiments, compare data, and interpret many of the observations, it is essential to use the appropriate coordinate system. The simplest system involves the geographic location, local time, and, on occasion, solar zenith angles. However, many of the high-latitude processes are greatly affected by the configuration of the magnetic field. Because of its importance and its complexity at Sondrestrom, it requires some discussion and a careful definition of magnetic coordinates.

The ability of the radar to observe an extended region, vertically and horizontally, is one of its strengths. Figure 1 shows the radar location and the extended volume it probes in terms of geographic and geomagnetic coordinates. The latter are derived from the IGRF (1980) model [IAGA, 1981] updated to 1983 and calculated for 350-km altitude. To observe the maximum possible range of geomagnetic latitude, the radar needs to observe in a plane that is nearly perpendicular to the lines of invariant latitude Λ, i.e., to the magnetic north. A close approximation to that, over much of the field of view, is at -27° geographic azimuth. Figure 2 shows geographic and geomagnetic coordinates in a vertical plane at that azimuth.

Paper number 4L6271.
0094-8276/84/004L-6271$03.00

A notable feature of the magnetic field is that magnetic north, i.e., the line perpendicular to invariant latitude, occurs at -27° azimuth, whereas the magnetic declination, commonly used for magnetic north, is at -39° azimuth. The magnetic declination is defined as the azimuth of a plane passing through the local magnetic field line and the local zenith. If the magnetic field were a centered dipole, then the two azimuths would be the same. If it were an offset dipole, then there would be only one plane for which the two azimuths would agree. Elsewhere, the magnetic meridian plane would be tilted with respect to the local zenith. For the real field, these parameters should rarely agree. At Sondrestrom, a tilt of only 2.1° is needed to account for a 12° difference between magnetic north and the magnetic declination.

To complement Λ in ordering the data, it is helpful to have an appropriate time parameter. The universal time (UT) and local standard time at Sondrestrom (midnight standard time is 0300 UT) are commonly used, but better parameters exist. However, they vary throughout the probed region. Midnight local solar time is 0324 UT at Sondrestrom and, referring to 350-km altitude in Figure 2, it varies with Λ from 35 min earlier at 64° to 50 min later at 82° . Similarily, midnight magnetic local time (MLT) is 0157 UT at Sondrestrom at equinox and varies from 14 min earlier at 64° to 30 min later at 82° . That this latter variation is not zero indicates that the plane at -27° is not exactly along the magnetic meridian, and that the meridian itself is not a plane.

The MLT is calculated according to a computer code developed by M. J. Baron and A. R. Hessing [SRI International, unpublished manuscript, 1982]. The geomagnetic field line is traced from the observed point until it intercepts the latitude of the subsolar point δ at geographic longitude λ_δ. The UT of magnetic midnight, expressed in degrees, is $360° - \lambda_\delta$ and each magnetic hour has 60 min. Magnetic midnight varies during the year as the subsolar latitude, or declination, varies. At Sondrestrom it is 15 min earlier at the winter solstice and 15 min later at the summer solstice, than at the equinoxes. All points along the same field line, as represented by the magnetic field model, will have the same MLT.

Because both Λ and MLT depend on the magnetic field, which is subject to secular variation; the constancy of these values has been examined. For 350 km above Sondrestrom, the IGRF model shows a reduction in Λ of 0.05° per year and an increase in the UT of magnetic midnight of 23 s per year. These extrapolated rates of change are small enough that for now, they can be neglected.

In addition to knowing what locations and times to associate with the data, knowing whether the region probed was sunlit is important. Because the radar is located just poleward of the arctic circle, the solar zenith angle (SZA) is always greater than 90° at the winter solstice and always less than 90° at the summer solstice. In Figure 3, SZA informa-

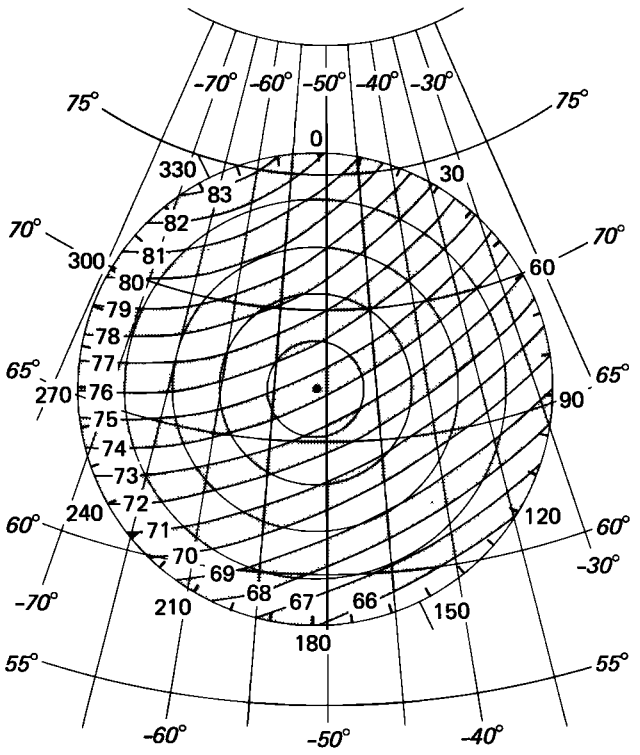

Fig. 1. Geographic and geomagnetic locations of Sondrestrom: Longitude and latitude, azimuth and distance (200-km intervals), invariant latitude from the IGRF (1980) model for 1983 and 350-km altitude.

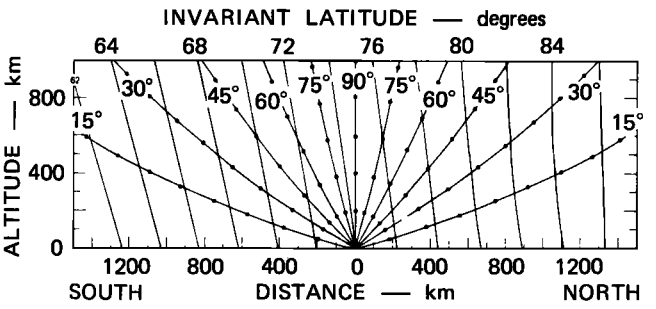

Fig. 2. Approximate magnetic meridian plane at -27° azimuth: Distance and altitude, elevation and range (200-km intervals), invariant latitude.

tion is displayed as a function of standard time at Sondrestrom and invariant latitude along the -27° azimuth. The sunlit region progresses from slightly south of the radar at noon at winter solstice to covering all but the southern part of the sky at midnight at summer solstice. A useful feature for comparison with radar observations is that in the morning and afternoon sectors the lines of constant SZA are roughly perpendicular to the lines of Λ.

Data Acquisition

Much of the region shown in Figures 1 and 2 has been probed using a general observational mode with a complex antenna pattern that is composed of three parts. The first is a multiposition pattern consisting of eleven fixed positions, which has evolved from the MITHRAS 1 mode used at Chatanika [Foster et al., 1981; de la Beaujardière et al., 1984]. There are five pairs of pointing directions symmetrically positioned in two planes 20° off vertical that intersect in a line at -27° azimuth. With this 40° angle between planes, pairs of points are 145 km apart at 200-km altitude or 358 km apart at 500 km. The pairs of pointing directions are at elevation angles of 30, 50, and 65° toward the north, and 30 and 50° toward the south. The remaining position is parallel to the local magnetic field. The second part consists of an elevation scan from 30° elevation in the south to 30° elevation in the north at 0.4° /s in the plane that passes through the geographic zenith and -27° azimuth. The third part consists of a similar elevation scan, but from east to west in the plane that passes through geographic zenith and is perpendicular to the previous scan.

In all three parts, data are obtained between approximately 80- and 550-km altitude. In the first and second parts, the observations span 72.5 to 75.5° invariant at 100-km altitude and 68 to 81° at 500 km. For a minimum elevation angle of 20° the observed region would be extended by a total of 2° at 100 km and 6° at 500 km.

While the data are recorded every 10 sec, the observing period is 15 min for the multiposition measurements and 5 min for each of the scans. The full cycle repeats every 27 min.

The physical parameters that can be derived from the radar data depend not only on the sequence of antenna positions, but also on the sequence of transmitted pulses and the sampling of the return signal. Many aspects of the radar system are described by Baron [1977], Kofman and Wickwar [1980], and Kelly [1983]. The major data acquisition program is described by Erb et al. [1981].

Because of the desire to observe a wide range of Λ and to look for the effects of low-energy particle precipitation, most of the emphasis has been on the F region. Therefore, most of the observations have been made with a 320-μs

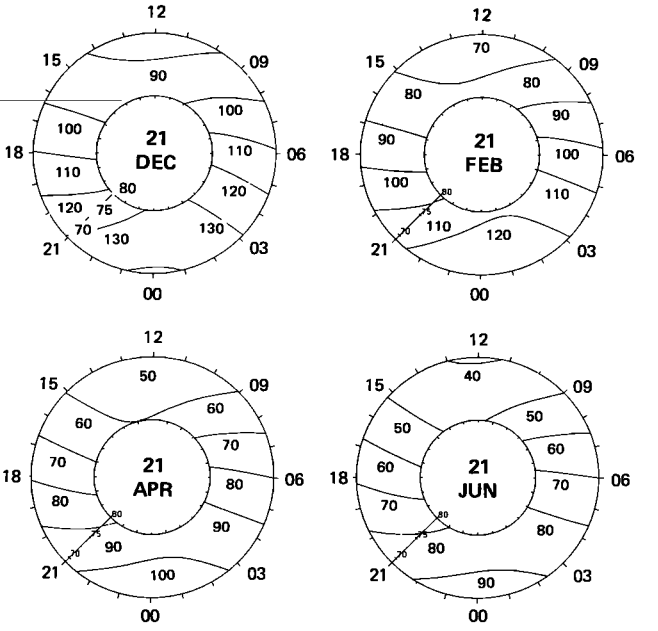

Fig. 3. Solar zenith angles over the radar field of view. The coordinates are invariant latitude, from 69° to 80° , at an azimuth of -27° and local standard time (add 3 hr for UT).

pulse. For a few experiments, a 60-μs pulse has been alternated with the long pulse thereby gaining more appropriate altitude resolution for the E region, but with loss of precision in the F region.

Derivation of Physical Parameters

The ability to derive an extensive list of physical parameters is one of the strengths of the radar technique. That ability has increased continuously since high-latitude observations began in 1971. Some of the procedures are described by de la Beaujardière et al. [1980]; however most are in specific research papers.

The backscattered power, primarily, provides information on electron densities. Much of the early work is discussed by Baron [1977] and references therein. From the E-region electron density profiles, the energy input from energetic particles is determined [Wickwar et al., 1975], as well as the spectrum of energetic electrons [Vondrak and Baron, 1976] and the accelerating potential [de la Beaujardière and Vondrak, 1982]. Corrections are needed for the E-region densities when large electric fields occur [Wickwar et al., 1981].

The Doppler shift of the return signal gives the ion velocity along the line of sight. After originally finding vector ion velocities or electric fields by combining three measurements [Doupnik et al., 1972], methods have been derived for finding them from measurements in one direction [de la Beaujardière et al., 1977] and over an extended latitude range from multiposition measurements [Foster et al., 1981]. The analysis of the latter was further refined during project MITHRAS and was adopted for the Sondrestrom 11-position data. For each of the three pairs of observing directions furtherest from the direction of the magnetic field, the velocity parallel to **B** is assumed zero and pairs of measurements are combined to find the velocity components perpendicular to **B**. For each of the two remaining pairs of observing directions, the measurement along **B** is included in the derivation of the velocity components perpendicular to **B**. In all cases, determination of the velocity components uses the calculated magnetic field at the points of observation.

The above density and velocity parameters have been combined to derive numerous electrodynamic parameters including conductivities, currents and Joule heating [Wickwar, 1975 and references therein], and Birkeland currents [Robinson et al., 1982].

The spectral information in the return signal gives the electron and ion temperatures in the F region [Kofman and Wickwar, 1980] and in the E region [Wickwar et al., 1981]. The analysis can be further refined to provide the atomic-to-molecular ion composition [Kelly and Wickwar, 1981] and at lower altitudes the ion-neutral collision frequency [Lathuillere et al., 1983]. In view of the large ion velocities often encountered at Sondrestrom, the analysis needs to be still further extended to find the ion composition under a greater variety of conditions.

The above densities and temperatures can be combined with the appropriate physics to determine additional physical parameters. These include the exospheric temperature [Kofman and Wickwar, 1984], the electron heat flux and energy loss rates [Kofman and Wickwar, 1984], the 4278-A intensity from N_2^+ [Wickwar et al., 1975], the 6300-A intensity from atomic oxygen [Wickwar and Kofman, 1984], the E-region neutral wind [Rino et al., 1977], and the F-region neutral wind in the magnetic meridian [Wickwar et al., 1984].

Summary

Because of its location, the large number of parameters deduced, and the extensive possiblities for correlative and coordinated measurements, data from the Sondrestrom radar will contribute significantly to our understanding of the flow of energy from the sun to the magnetosphere, ionosphere and neutral atmosphere as well as to our understanding of the interactions among these regions.

Acknowledgments. We thank the many people in Menlo Park and Sondrestrom who contribute to the operation of the radar and analysis of the data. The Sondrestrom radar is operated by SRI International under NSF cooperative agreement ATM8121671.

References

Baron, M. J., The Chatanika Radar System, in *Radar Probing of the Auroral Plasma,* edited by A. Brekke, pp. 103-141, Universitetsforlaget, Tromso, Norway, 1977.

de la Beaujardière, O., and R. R. Vondrak, Chatanika radar observations of the electrostatic potential distribution of an auroral arc, *J. Geophys. Res., 87,* 797-809, 1982.

de la Beaujardière, O., R. R. Vondrak, and M. J. Baron, Radar observations of electric fields and currents associated with auroral arcs, *J. Geophys. Res., 82,* 5051-5062, 1977.

de la Beaujardière, O., V. B. Wickwar, M. J. Baron, J. Holt, R. M. Wand, W. L. Oliver, P. Bauer, M. Blanc, C. Senior, D. Alcayde, G. Caudal, J. Foster, E. Nielsen, and R. Heelis, MITHRAS: A brief description, *Radio Sci., 19,* 665-673, 1984.

de la Beaujardière, O., V. B. Wickwar, C. A. Leger, M. McCready, and M. J. Baron, The software system for the Chatanika incoherent scatter radar, Technical Report, pp. 117, SRI International, Menlo Park, CA 1980.

Doupnik, J. R., P. M. Banks, M. J. Baron, C. L. Rino, and J. Petriceks, Direct-measurement of plasma drift velocities at high magnetic latitudes, *J. Geophys. Res., 77,* 4268-4271, 1972.

Erb, D., C. H. Dawson, and M. Lemmons, Operating manual for the Chatanika/ Sondrestrom radar data acquisition system — Hatol, Technical Report, pp. 56, SRI International, Menlo Park, CA, 1981.

Foster, J. C., J. R. Doupnik, G. S. Stiles, Large scale patterns of auroral ionospheric convection observed with the Chatanika radar, *J. Geophys. Res., 86,* 11357-11371, 1981.

IAGA Division 1, Working Group 1, International geomagnetic reference fields: DGRF 1965, DGRF 1970, DGRF 1975, and IGRF 1980, *EOS Transactions AGU, 62,* 1169, 1981.

Kelly, J. D., Sondrestrom radar — initial results, *Geophys. Res. Lett., 10,* 1112-1115, 1983.

Kelly, J. D., and V. B. Wickwar, Radar measurements of

high-latitude ion composition between 140 and 300 km altitude, *J. Geophys. Res., 86,* 7617-7626, 1981.

Kofman, W., and V. B. Wickwar, Plasma line measurements at Chatanika with high-speed correlator and filter bank, *J. Geophys. Res., 85,* 2998-3012, 1980.

Kofman, W., and V. B. Wickwar, Very high electron temperatures in the daytime F region at Sondrestrom, *Geophys. Res. Lett.,* this issue, 1984.

Lathuillere, C., V. B. Wickwar, and W. Kofman, Incoherent scatter measurements of ion-neutral collision frequencies and temperatures in the lower thermosphere of the auroral region, *J. Geophys. Res., 88,* 10,137-10,144, 1983.

Rino, C. L., A. Brekke, and M. J. Baron, High-resolution auroral zone E region neutral wind and current measurements by incoherent scatter radar, *J. Geophys. Res., 82,* 2295-2304, 1977.

Robinson, R. M., R. R. Vondrak, and T. A. Potemra, Electrodynamic properties of the evening sector ionosphere within the Region 2 field-aligned current sheet, *J. Geophys. Res., 87,* 731-741, 1982.

Vondrak, R. R., and M. J. Baron, Radar measurements of the latitudinal variations of auroral ionization, *Radio Sci., 11,* 939-946, 1976.

Wickwar, V. B., Chatanika Radar Measurements, in *Atmospheres of Earth and The Planets,* edited by B. M. McCormac, pp. 111-124, D. Reidel, Boston, MA, 1975.

Wickwar, V. B., M. J. Baron, and R. D. Sears, Auroral energy input from energetic electrons and Joule heating at Chatanika, *J. Geophys. Res., 80,* 4364-4367, 1975.

Wickwar, V. B., and W. Kofman, Dayside red auroras at very high latitudes: The importance of thermal excitation, *Geophys. Res. Lett.,* this issue, 1984.

Wickwar, V. B., C. Lathuillere, W. Kofman, and G. Lejeune, Elevated electron temperatures in the auroral E layer measured with the Chatanika radar, *J. Geophys. Res., 86,* 4721-4730, 1981.

Wickwar, V. B., J. W. Meriwether, Jr., P. B. Hays, and A. F. Nagy, The meridional thermospheric neutral wind measured by radar and optical techniques in the auroral region, *J. Geophys. Res.,* in press, 1984.

V. B. Wickwar, J. D. Kelly, O. de la Beaujardière, C. A. Leger, F. Steenstrup, and C. H. Dawson, SRI International, Radio Physics Laboratory, 333 Ravenswood Avenue, Menlo Park, CA 94025.

(Received July 3, 1984;
accepted August 7, 1984.)